Nuclear Instruments and Methods in Physics Research A 623 (2010) 1024–1029

Contents lists available at ScienceDirect

Nuclear Instruments and Methods in Physics Research A

journal homepage: www.elsevier.com/locate/nima

The stability of TlBr detectors at low temperature

Burçin Dönmez [a,*], Zhong He [a], Hadong Kim [b], Leonard J. Cirignano [b], Kanai S. Shah [b]

[a] Department of Nuclear Engineering and Radiological Sciences, University of Michigan, Ann Arbor, MI 48109, USA
[b] Radiation Monitoring Devices Inc., Watertown, MA 02472, USA

ARTICLE INFO

Article history:
Received 11 July 2010
Received in revised form
6 August 2010
Accepted 9 August 2010
Available online 4 September 2010

Keywords:
Thallium bromide
TlBr
Semiconductor detector

ABSTRACT

Thallium bromide (TlBr) is a promising semiconductor detector material due to its high atomic number (Tl: 81, Br: 35), high density (7.56 g/cm^3) and wide band gap (2.68 eV). Current TlBr detectors suffer from polarization, which causes performance degradation over time when high voltage is applied. A 4.6-mm thick TlBr detector with pixellated anodes made by Radiation Monitoring Devices Inc. was used in the experiments. The detector has a planar cathode and nine anode pixels surrounded by a guard ring. The pixel pitch is 1.0-mm. Digital pulse waveforms of preamplifier outputs were recorded using a multi-channel GaGe PCI digitizer board for pulse shaping. Several experiments were carried out at $-20\,^{\circ}$C while the detector was under bias for over a month. No polarization effect was observed and the detector's spectroscopic performance improved over time. Energy resolution of 1.5% FWHM at 662 keV has been measured without depth correction at -2000 V cathode bias. Average electron mobility-lifetime of $(5.7 \pm 0.8) \times 10^{-3}$ cm^2/V has been measured from four anode pixels.

1. Introduction

Thallium bromide (TlBr) is a promising new semiconductor detector material for X- and gamma-ray applications for homeland security, astrophysics and medical imaging. It has a high gamma-ray stopping power due to its high density (7.56 g/cm^3) and high atomic number (Tl: 81, Br: 35). Also, its wide band gap (2.68 eV) makes it very suitable for room-temperature operation.

However, current TlBr detectors suffer from polarization effects which degrade spectroscopic performance over time when bias voltage is applied. It has been suggested in Ref. [1] that ionic conductivity causes polarization in TlBr detectors. By applying bias voltage, Tl^+ and Br^- ions are accumulated under the cathode and anode electrodes, respectively [2]. This causes a degradation in the electric-field intensity inside the detector; i.e. the polarization effect, and therefore signal amplitude reduces over time until complete breakdown of the electric field. It is shown that the polarization effect in TlBr detectors can be suppressed with Tl electrodes coated by Au contacts [2]. The polarization effect is also partially mitigated by reversing the polarity of the high bias applied to the detector [3]. It is shown in Ref. [4] that no polarization effect is observed with TlBr detectors at $-20\,^{\circ}$C when high bias is applied for over 5 days.

In this work, a 4.6-mm thick TlBr detector was kept under bias for over a month at $-20\,^{\circ}$C and digital waveforms were recorded from four anode pixels and the cathode for spectroscopy measurements. The detector was stable over the measurement time.

2. Experimental setup

The detector studied is a 4.6-mm thick pixellated TlBr detector with Au/Cr contacts manufactured by Radiation Monitoring Devices Inc. The cathode is a planar electrode, while the anode has nine pixels with 1.0-mm pitch surrounded by a guard ring. The detector is placed inside a test box with five readout channels and connected to charge-sensitive Amptek A250 preamplifiers for readout. Digital pulse waveforms from four anode pixels and the cathode were recorded using a 14-bit GaGe Octopus CompuScope PCI bus on a personal computer. Each pulse waveform (or event) per channel has 512 points sampled every 100 ns. Example waveforms for a photopeak event close to the cathode surface for a typical anode pixel and the cathode can be seen in Fig. 1. The drop of the signal amplitude is due to the time constant of the preamplifier used in the detection system.

Recorded waveforms for each channel were analyzed with software written in MATLAB [5] and ROOT [6]. For this analysis, a digital CR-RC shaping filter with 10-μs shaping time for anode signals and 24-μs shaping time for the cathode signal was used. Shaping time for the signals was kept long to avoid ballistic deficit since mobility of charge carriers is very low in TlBr.

The detector test box was placed inside a temperature chamber where it was kept at $-20\,^{\circ}$C during the experiments.

* Corresponding author.
E-mail address: burcind@umich.edu (B. Dönmez).

0168-9002/$ - see front matter © 2010 Elsevier B.V. All rights reserved.
doi:10.1016/j.nima.2010.08.024

3. Experimental results

3.1. Spectroscopic performance at −500 V

Several experiments were carried out at −20 °C with a ^{137}Cs source. Digital waveforms from four anode pixels and the cathode were recorded and analyzed. At the beginning, the detector was biased up to −500 V for spectroscopy measurements and data were collected for a period of 16 h. Fig. 2 shows a typical anode pixel spectrum and depth-separated spectrum using the cathode-to-anode signal ratio [7,8]. Poor spectroscopic performance of the anode pixel was attributed to the severe electron trapping, shown on the right-hand side of Fig. 2. After this observation, experiments were stopped and the detector was biased down. This experiment was repeated more than a month later and similar results were obtained.

3.2. Spectroscopic performance at −1000 V

After observing poor spectroscopic performance at −500 V, the detector's bias was increased to −1000 V. The effect of electron trapping was greatly reduced and the detector's spectroscopic performance improved significantly. Fig. 3 shows a typical anode pixel spectrum and depth separated spectrum using the cathode-to-anode signal ratio measured at −1000 V. The depth separated spectrum also implies that at this voltage the detector was fully active in all depths. For pixel 5, measured energy resolution was 2.7% FWHM at 662 keV without depth correction.

The detector was kept under bias and more data were collected during the following weeks. After two weeks, measured spectroscopic performance showed an improvement, as shown in Fig. 4. For pixel 5, measured energy resolution was 2.3% FWHM at 662 keV. No depth correction is applied to the data. This result is very encouraging and suggests that TlBr detectors can be operated for a long period of time at low temperatures without significant polarization effects. Spectroscopic performance of the detector also improved over time. Stability of the detector and detailed comparison of results at −1000 V will be discussed later.

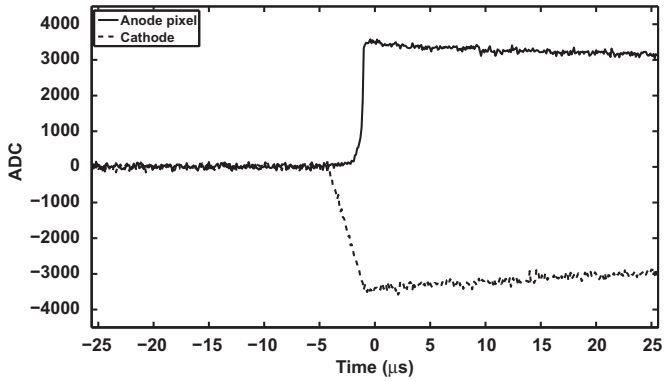

Fig. 1. Typical anode pixel and cathode waveforms for a photopeak event close to the cathode surface with a ^{137}Cs source and −2000 V bias.

3.3. Spectroscopic performance at −2000 V

The detector bias was gradually increased to −2000 V and kept at this bias for about two more weeks. Fig. 5 shows raw anode-pixel spectra without any depth correction for four pixels at −2000 V with a ^{137}Cs source. Measured energy resolution was 2.7%, 4.2%, 2.9% and 1.5% FWHM at 662 keV for pixels 1, 2, 4 and 5, respectively. These results were obtained with the last data set taken during continuous operation of the detector over a month at −20 °C.

3.4. Stability of the detector

The polarization effect in TlBr detectors appears in the energy spectrum as changes in energy resolution, photopeak amplitude and photopeak efficiency. The change in these parameters as a function of time is investigated in this section.

Figs. 6, 7 and 8 compare changes of photopeak pulse amplitude, energy resolution and number of total and photopeak events for two data sets collected at −1000 V two weeks apart from each other. It can be seen clearly in Fig. 6 that photopeak

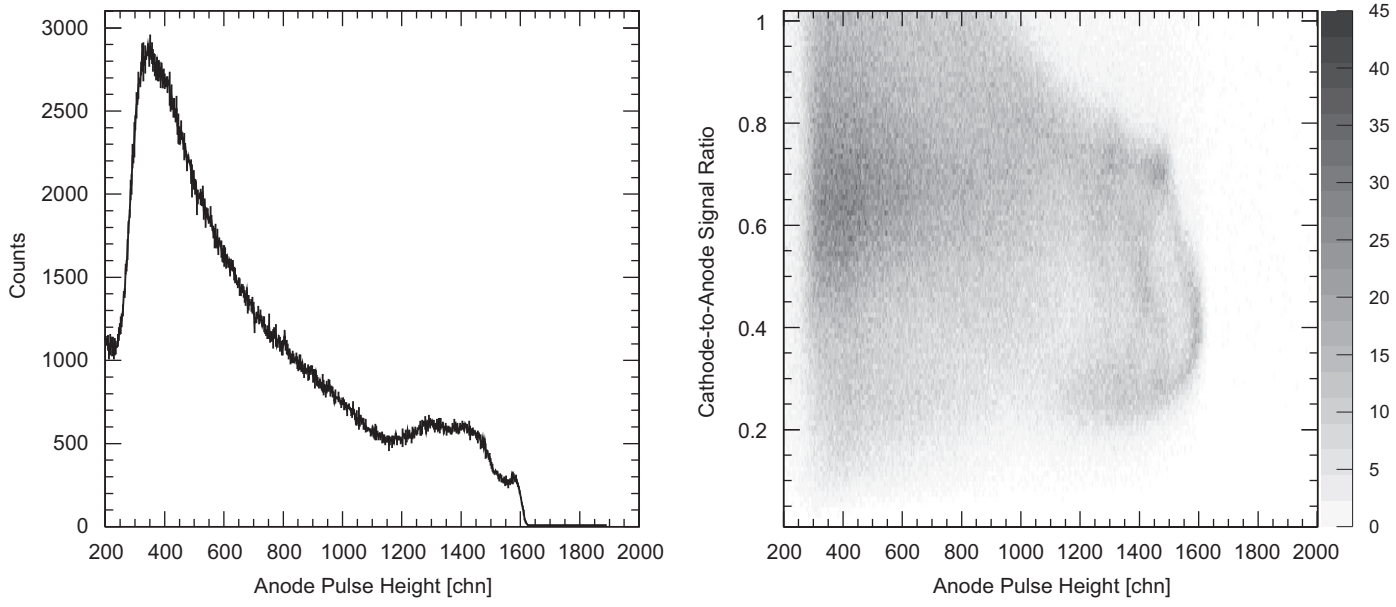

Fig. 2. ^{137}Cs raw anode pixel spectrum (left) and depth-separated spectrum (right) using the cathode-to-anode ratio at −500 V bias. Higher cathode-to-anode ratios correspond to interactions near the cathode surface. Severe electron trapping is observed. Data were collected at −20 °C.

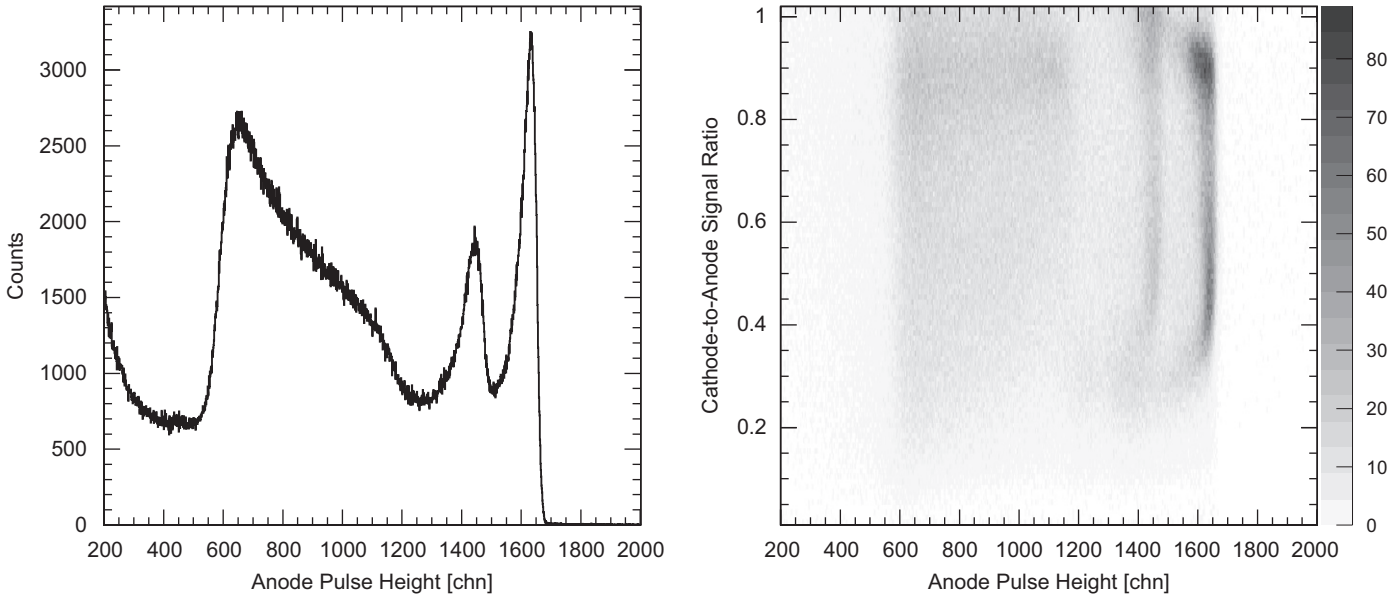

Fig. 3. ^{137}Cs raw anode pixel spectrum (left) and depth-separated spectrum (right) using the cathode-to-anode ratio at −1000 V bias. The smaller peak located at the lower energy side of the 662 keV (i.e., channel ~1620) peak is the Tl X-ray escape peak. Higher cathode-to-anode ratios correspond to interactions near the cathode surface. For pixel 5, measured energy resolution was 2.7% FWHM at 662 keV. Data were collected at −20 °C.

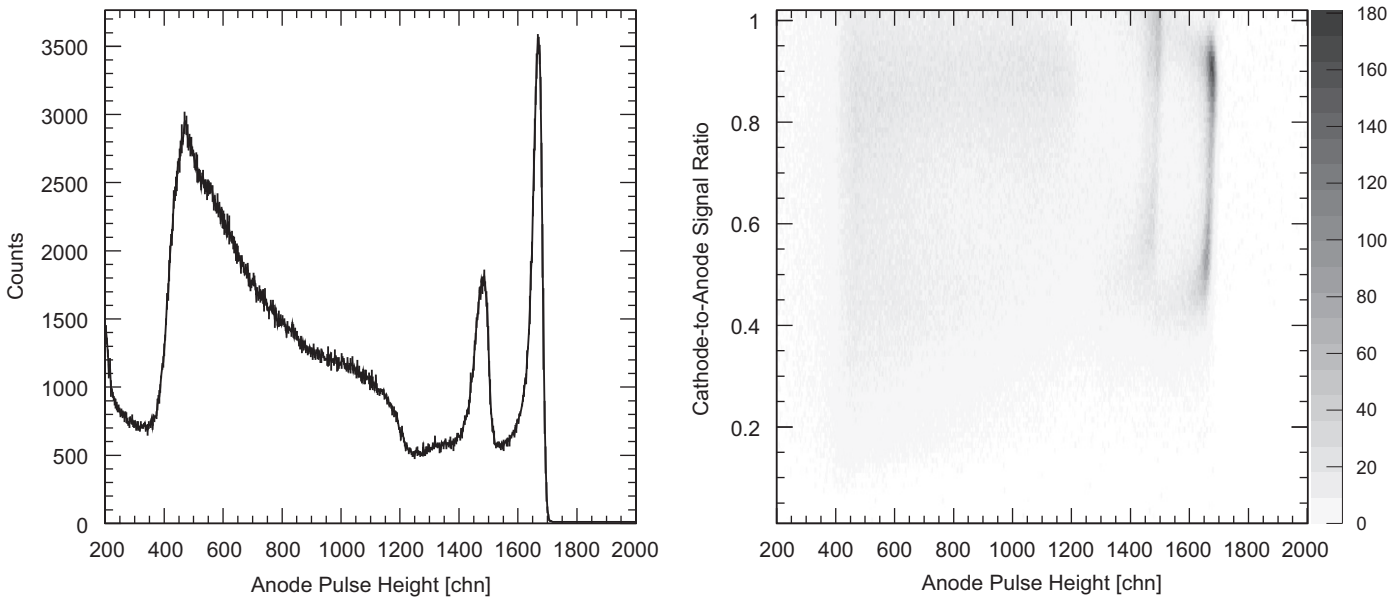

Fig. 4. ^{137}Cs raw anode pixel spectrum (left) and depth-separated spectrum (right) using the cathode-to-anode ratio at −1000 V bias. Higher cathode-to-anode ratios correspond to interactions near the cathode surface. For pixel 5, measured energy resolution was 2.3% FWHM at 662 keV. Data were collected at −20 °C two weeks after the first data set shown in Fig. 3.

amplitude stayed almost constant over time for all anode pixels and for the cathode. A small change in amplitude of the signals, especially for the cathode signal, was observed on the first data set. This was attributed to the detector becoming conditioned over time. Energy resolution for each pixel did not show any significant degradation over time. In fact, uncorrected energy resolution improved after two weeks for all anode pixels, except for pixel 1, as shown in Fig. 7. In Fig. 8, comparison of the two data sets shows reduction in the variation of photopeak efficiency for each pixel over time. This is another indication of the stability improvement of the detector over time. One of the interesting observations is that photopeak efficiency for some of the anode pixels improved over time.

3.5. Electron mobility-lifetime

The method proposed in Ref. [9] was used to calculate electron mobility-lifetime ($\mu_e\tau_e$) product. This method relies on measuring photopeak amplitudes for events close to the cathode surface at two different cathode biases. The photopeak amplitudes are proportional to the number of electrons collected at the anode

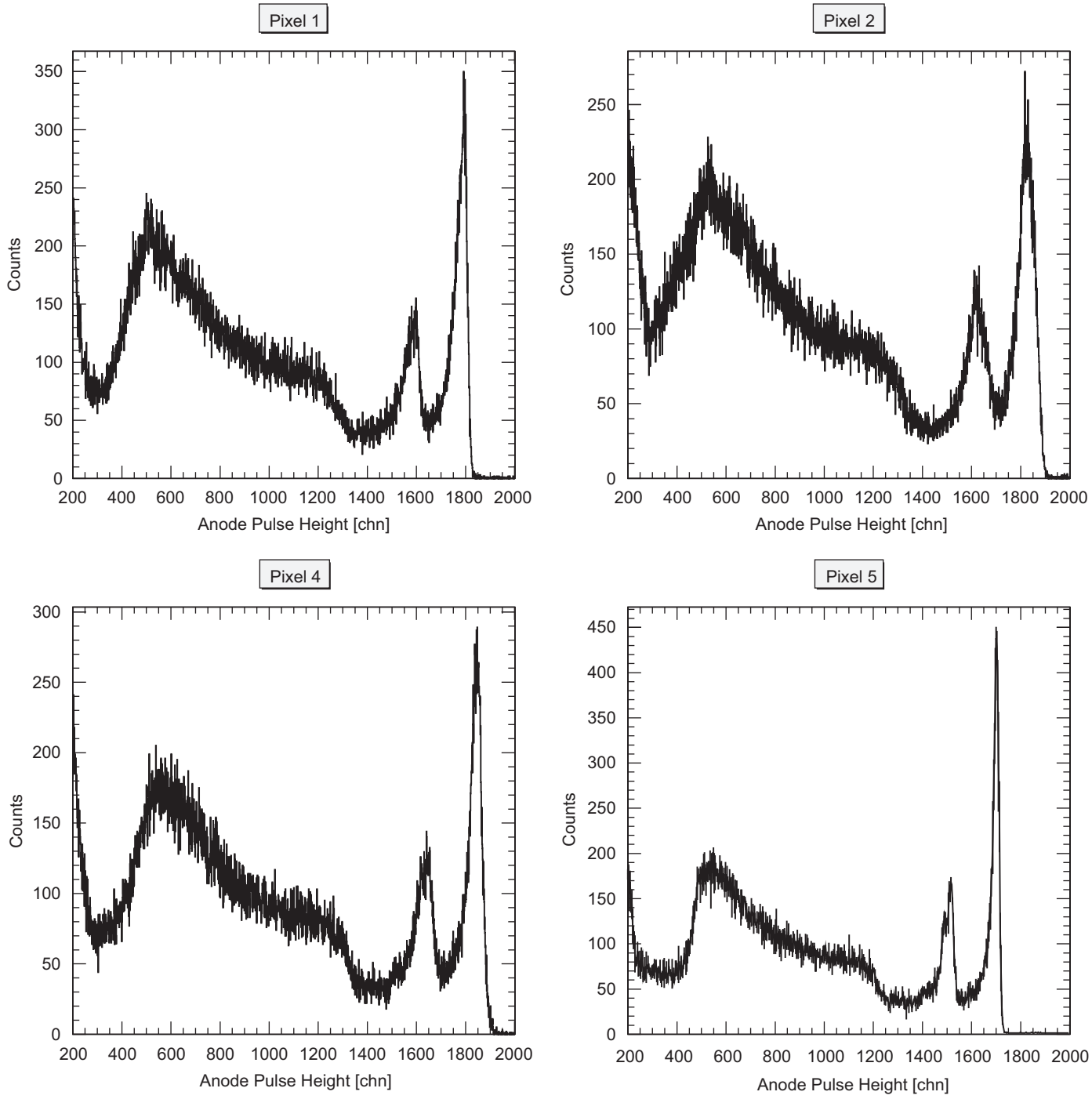

Fig. 5. ^{137}Cs raw anode-pixel spectra at -2000 V bias. Measured energy resolution was 2.7%, 4.2%, 2.9% and 1.5% FWHM at 662 keV for pixels 1, 2, 4 and 5, respectively. No depth correction was applied. Data were collected at $-20\,^{\circ}$C.

pixel and the number of electrons is proportional to the applied bias with single polarity charge sensing detectors. The electron mobility-lifetime can be found using the following equation:

$$\mu_e\tau_e = \frac{D^2}{\ln(N_1/N_2)}\left(\frac{1}{V_2}-\frac{1}{V_1}\right) \quad (1)$$

where D is the detector thickness, N_1 and N_2 are the photopeak centroids under two different cathode biases, V_1 and V_2. Energy spectra with a ^{137}Cs source were collected at two different cathode biases, -1000 and -2400 V. Then, $\mu_e\tau_e$ was calculated for each pixel using Eq. (1). Results of calculated $\mu_e\tau_e$ can be seen in Table 1 for all anode pixels that were tested. Average electron mobility-lifetime was calculated to be $(5.7\pm0.8)\times10^{-3}$ cm^2/V.

4. Discussion and future work

A 4.6-mm thick TlBr detector made by Radiation Monitoring Devices Inc. successfully operated under bias for over a month at $-20\,^{\circ}$C. Energy resolution of 1.5% with a ^{137}Cs source was obtained for the best anode pixel without any depth correction at -2000 V.

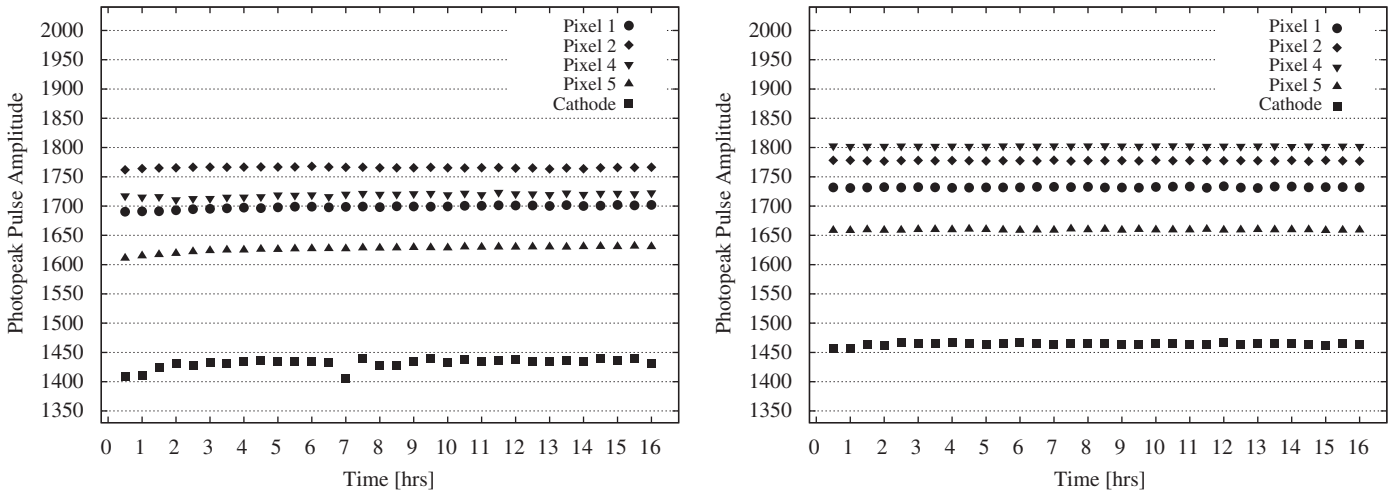

Fig. 6. Photopeak pulse amplitudes for all anode pixels and the cathode at −1000 V with ^{137}Cs on two different dates. Data shown on the left figure were taken two weeks before data shown on the right figure.

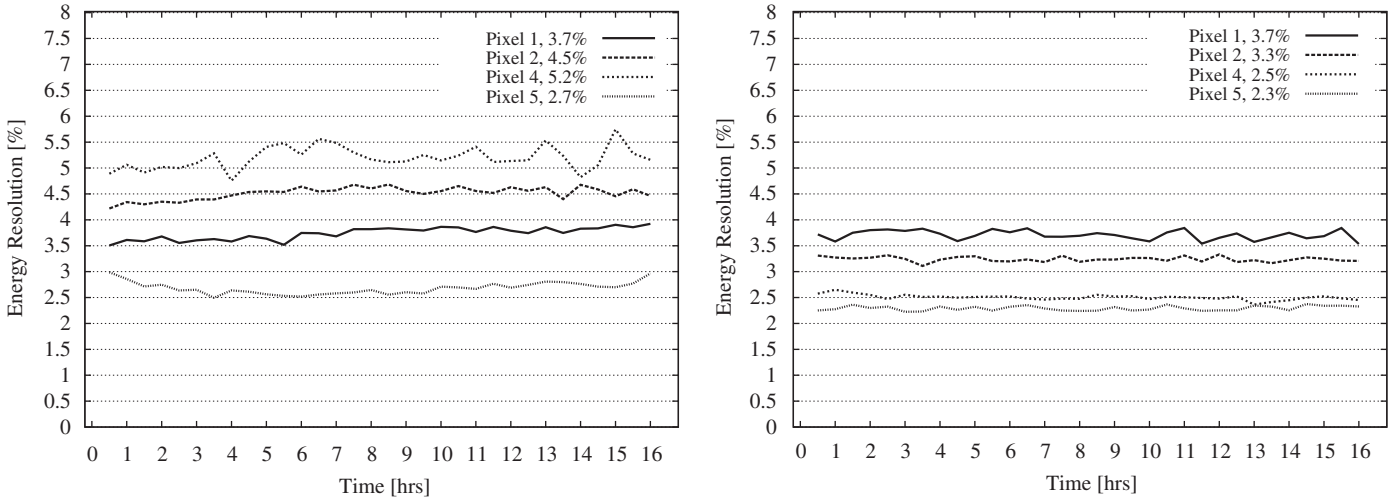

Fig. 7. Energy resolution in FWHM over time with ^{137}Cs (662 keV) at −1000 V on two different dates. Data shown on the left figure were taken two weeks before data shown on the right figure. No depth correction was applied to either data set.

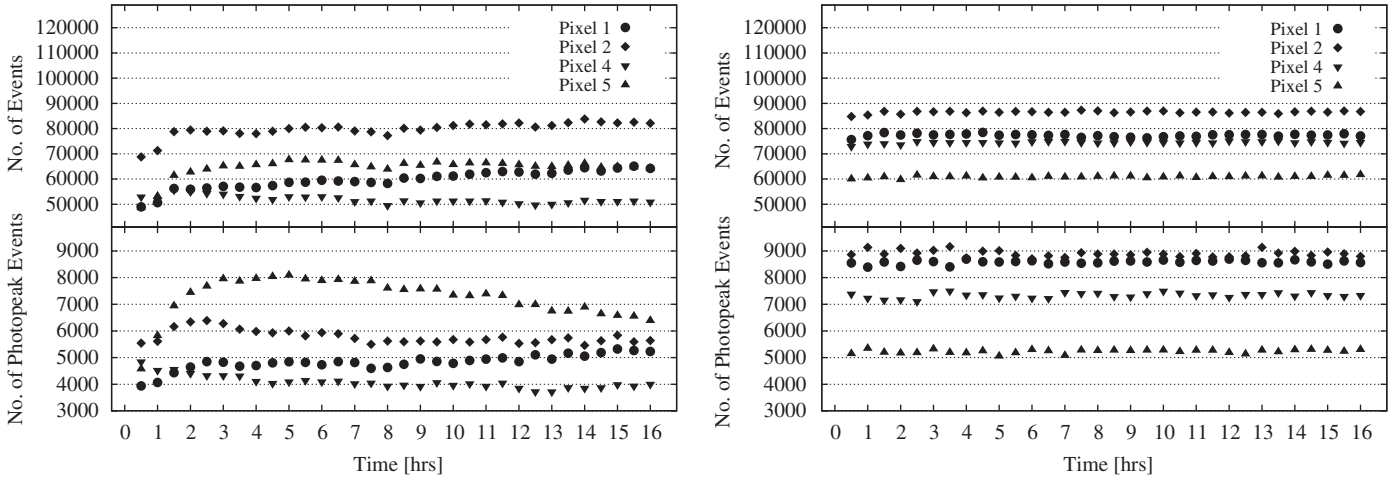

Fig. 8. Number of total events and number of photopeak events in each pixel at −1000 V on two different dates. Data shown on the left figure were taken two weeks before data shown on the right figure.

Table 1
Calculated $\mu_e\tau_e$ for all pixels that were tested.

Pixel number	$\mu_e\tau_e$ ($\times 10^{-3}$ cm^2/V)
1	5.9
2	4.6
4	5.7
5	6.4

Data sets were collected two weeks apart at -1000 V. These data showed that photopeak amplitudes stayed constant within the same experiment. An average increase of 2.5% in the gain of the anode pixels was observed when comparing these two data sets. Improvement in the energy resolution was also observed. Some irregularities of photopeak efficiency were observed in the first data set at -1000 V. This is likely due to conditioning of the detector to the applied bias.

Average electron mobility-lifetime was calculated to be $(5.7 \pm 0.8) \times 10^{-3}$ cm^2/V. This shows that the electron transport properties are similar to those measured in CdZnTe.

The effect of different operating temperatures on the detector's performance will be studied in greater detail using this detector in the future.

Acknowledgments

This work is supported by the U.S. Department of Homeland Security, Domestic Nuclear Detection Office.

Burçin Dönmez would like to thank Miesher L. Rodrigues and Willy R. Kaye of the University of Michigan for their helpful discussions and suggestions. The authors would also like to thank Christopher G. Wahl of the University of Michigan for proof-reading the manuscript.

References

[1] V. Kozlov, M. Kemell, M. Vehkamäki, M. Leskelä, Nucl. Instr. and Meth. A 576 (2007) 10.
[2] K. Hitomi, T. Shoji, Y. Niizeki, Nucl. Instr. and Meth. A 585 (2008) 102.
[3] B. Dönmez, S.E. Anderson, Z. He, L.J. Cirignano, H. Kim, K.S. Shah, in: IEEE NSS/MIC Conference Record, 2008, pp. 291–293.
[4] T. Onodera, K. Hitomi, T. Shoji, Nucl. Instr. and Meth. A 576 (2006) 433.
[5] ⟨http://www.mathworks.com⟩.
[6] ⟨http://root.cern.ch⟩.
[7] Z. He, G.F. Knoll, D.K. Wehe, R. Rojeski, C.H. Mastrangelo, M. Hammig, C. Barrett, A. Uritani, Nucl. Instr. and Meth. A 380 (1996) 228.
[8] Z. He, G.F. Knoll, D.K. Wehe, J. Miyamoto, Nucl. Instr. and Meth. A 388 (1997) 180.
[9] Z. He, G.F. Knoll, D.K. Wehe, J. Appl. Phys. 84 (1998) 5566.